euspen's 26th International Conference & Exhibition, Krakow, PL, June 2026
www.euspen.eu

Surface Analysis and Evaluation of Corrosion-Induced and Pore-Like Textures

Aleksandra Mirowska[1,2], Robert Tomkowski[2], Michał Dobrzyński[1], Amir Rashid[2], Sasan Dadbakhsh[2]

[1]*Faculty of Mechanical Engineering and Ship Technology, Gdansk University of Technology, Narutowicza 11/12,80-233 Gdansk, Poland*
[2]*Department of Production Engineering, KTH Royal Institute of Technology, Brinellvägen 68, 114 28 Stockholm, Sweden*

aleksandra.mirowska@pg.edu.pl

Abstract
Surfaces exhibiting corrosion degradation effects and similar pore structures present complex topographical features that significantly influence material performance and durability. This study develops and evaluates comprehensive measurement methodologies for characterising surfaces displaying both corrosion-induced degradation patterns and analogous pore-like structural features. Using integrated optical profilometry, scanning electron microscopy (SEM) and three-dimensional (3D) surface reconstruction techniques, surfaces were systematically analysed for their morphological characteristics. Key parameters including pore/pit size distribution, surface roughness metrics, texture similarity indices, and topographical complexity were quantitatively assessed across multiple sample conditions. The analysis reveals that corrosion-damaged surfaces and engineered pore structures exhibit comparable textural signatures with distinguishable differences in feature organisation and spacing patterns. A standardised evaluation protocol was developed to objectively measure and classify these corrosion-like surface textures based on morphological parameters and spatial characteristics. The proposed framework enables reliable differentiation and quantitative assessment of corroded versus artificially created pore-textured surfaces. The results demonstrate practical applications for surface quality control and corrosion monitoring. This work provides essential methodology for consistent reproducible evaluation of complex corrosion and pore-structured surfaces in materials science and industrial applications.

Surface porosity measurement, corrosion-like surfaces, 3D topography characterization, surface roughness evaluation

1. Introduction

Material surfaces exhibiting corrosion and porous structures are a key focus of modern materials science due to their complex topography, which has a significant impact on the properties and durability of the material. Both natural processes, such as corrosion degradation, and manufacturing technologies generate an irregular distribution of pits, pores and peaks with a multi-dimensional distribution characterised by high spatial variability [1]. Corrosion processes result in deep, localized pits (pitting corrosion) with highly irregular morphology, ranging from a few to tens of micrometers in diameter, with depths often exceeding 10 µm [2]. The distribution of pits on the surface is subject to statistical fluctuations, and in long-term potentiodynamic tests, it takes the form of irregular, branching structures. This topography symptomatically contains bimodal height distributions: pit bottoms (local depths of several micrometers) and the core of the surface between pits, which is reflected in the roughness parameters. Surfaces produced using laser powder bed fusion (LPBF), due to the high temperatures involved in the process, are characterised by a topography consisting of regularly spaced peaks and valleys, and also contain surface and subsurface pores comparable in size to corrosion pits [3]. Such topography has a significant impact on the functional properties of the materials [4]. In the case of highly complex surfaces, traditional two-dimensional roughness parameters (Ra, Rz) are insufficient [5,6]. In the last two decades, with the development of optical profilometry methods and the standardisation of three-dimensional surface texture parameters in ISO 25178, there has been a transformation in the approach to characterising topography [7]. The methodological challenge is to develop reliable, repeatable characterisation procedures that would enable objective characterisation of such complex surfaces [8–10].

Focus Variation (FV) is a non-contact method of 3D optical profilometry based on sequential image acquisition at different focus distances and identification of the maximum contrast corresponding to the surface topography. The choice of lens magnification is a fundamental metrological challenge due to the interrelationships between depth of field (DOF), lateral resolution, field of view and measurement reliability. Rojewski [11] in his work on non-alloy steel surface stated that the microscope magnification plays a critical role in the accuracy of the surface topography representation. Depth of field is inversely proportional to the square of the numerical aperture ($DOF \propto \lambda/NA^2$), which means that at low magnification (5×) it is several tens of micrometres, while at high magnification (50×) it is only a few micrometres [12]. A wide DOF at low magnification generates flat, multimodal contrast functions, preventing the algorithm from accurately determining the topography, especially in low-contrast areas, resulting in higher fraction of non-measured points (NMPs). Narrow DOF at high magnification produces sharp, single-peak contrast features, enabling reliable topography identification and reducing NPMs. The pixel size varies from 3–5 µm at 5× to 0.3–0.5 µm at 50×, which radically affects the representation of topography: at low magnification, pores are underrepresented, reducing their amplitude, while at high magnification they occupy hundreds of pixels. However, the use of low-magnification objective lenses allows for imaging of a larger area, which can provide a better view of the textures being investigated. Some studies show that the amplitude parameters decrease significantly when switching objective lenses from 5× to 50× [13]. The field of view decreases proportionally to the magnification, limiting the sampling area, while the resolution in the Z direction improves from low

magnification to high magnification. Surface texture contrast also plays a key role – at low magnification, the number of pixels representing the structure is small, reducing the possibility of signal averaging, while at high magnification, hundreds of pixels allow for better integration and noise resistance. Choosing the optimal magnification therefore requires a careful compromise between reducing NMPs, improving resolution, narrowing the field of view, and possible inaccuracies in the amplitude of roughness parameters.

The aim of this study is to systematically evaluate the impact of lens magnification (5×, 10×, 20×, 50×) on surface roughness parameters and the percentage of non-measured points (NMPs) for corroded 316L steel samples and laser powder bed fusion Osprey® HWTS 50 tool steel samples, in order to develop a standardised protocol for reliable and repeatable characterisation of complex topographies in materials science and industrial applications.

2. Methodology

2.1. Samples preparation

In this study, two types of porous surfaces were prepared: 316L steel subjected to potentiodynamic tests and laser powder bed fusion (LPBF) tool steel samples.

For the corrosion tests, the disc-shaped samples with an exposure area of 1 cm² were wet-ground to a final gradation of #2000. The samples were cleaned and degreased using isopropanol with 99.7% purity (POCH, Poland). Electrochemical tests were performed using potentiostat/galvanostat (Atlas 0531, Atlas Sollich, Poland) in NaCl (99.8% purity, Warchem, Poland) solutions of 3.5, 10 and 20 wt(%) to obtain low, medium and high porosity surfaces, respectively (CORR_LOW, CORR_MEDIUM, CORR_HIGH samples). A three-electrode setup was employed, consisting of a platinum electrode as the counter electrode, a saturated calomel electrode as the reference electrode, and aluminum samples as the working electrode. The measurements began with determining the open circuit potential (OCP) over 30 min. Corrosion process were obtained using the potentiodynamic tests over a potential range of -2 V to + 1 V, with a scanning rate of 1 mV/s. After testing, salt deposits were removed from the tested surfaces by cleaning in an ultrasonic cleaner (MKD-6, MKD ULTRASONIC, Poland).

For manufacturing the LPBF samples, a mixture of metal powder and a binder was provided to create a more emphasized surface roughness in the form of a semi-fluid paste. In the paste mixture, the metal powder were spherical in a size range between (15-45microns) from tool steel Osprey® HWTS 50. Then, 40g of the tool steel powder was mixed with 1.1g of corn starch dissolving in 5ml of water (mixing was done when water was boiled). This formulation allowed adequate binding strength to maintain layer cohesion while ensuring the paste could be applied uniformly across the base plate. Afterwards, a layer of paste is applied manually on a still base plate and then the applied layer was moved into a EOS M270 laser powder bed fusion additive manufacturing machine. In the laser powder bed fusion machine, the applied layer was scanned as 10mm*10mm squares with a fibre laser using a laser power of 100W, a scanning velocity of 75-800 mm/s and a hatch spacing of 0.1 mm. This procedure was manually repeated layer-by-layer until 1-2 mm tool still parts were made. This procedure allowed to obtain LPBF_LOW, LPBF_MEDIUM and LPBF_HIGH samples.

2.2. Scanning Electron Microscopy observations

All of the obtained surfaces were observed using scanning electron microscopy (SEM) operating at an accelerating voltage of 10 kV (Tescan Vega G4, Czech Republic). A magnification of 100x was applied.

2.3. Surface measurements

The topography of the resulting surfaces was characterized using a 3D optical profilometer based on FV microscopy (Sensofar S Neox, Sensofar Metrology, Terrassa, Spain). Nikon EPI objectives with magnifications of 5×, 10×, 20×, and 50× were employed, and the data were initially processed using SensoSCAN S Neox 7.7 software. The technical specifications of the lenses are summarized in Table 1. For each sample, three randomly selected areas were analyzed. Fig. 1 presents a schematic representation of the analyzed regions and their dimensions for the different objective magnifications applied in the study. Surface analysis was subsequently carried out using SensoMAP Premium 9.1 software. The procedure used to determine the required parameters was in accordance with the ISO 25178 and ISO 21920 standards.

Table 1. Objective lenses properties on Sensofar S Neox 7 optical profilometer.

Magnification	5x	10x	20x	50x
NA	0.15	0.30	0.45	0.8
WD [mm]	23.50	17.50	4.50	1.00
FOV [µm x µm]	3378 x 2826	1689 x 1413	845 x 707	338 x 283
Spatial sampling [µm]	1.38	0.69	0.34	0.13
Optical resolution [µm]	1.08	0.54	0.36	0.20

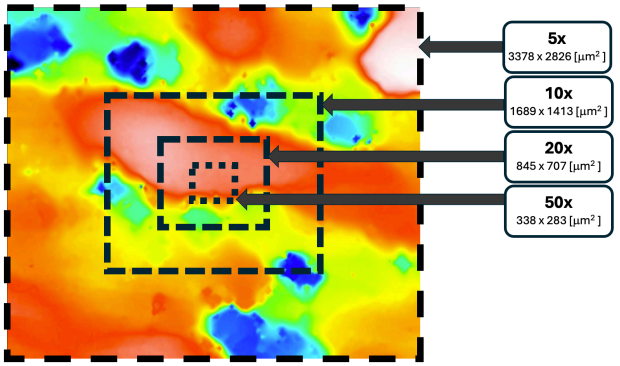

Figure 1. Schematic representation of the selection of measurement areas and locations. Based on the example of LPBF_HIGH surface.

3. Results and Discussion

Fig. 2 shows images of samples obtained with a scanning electron microscope. It can be observed that both surfaces subjected to corrosion processes and those produced by the LPBF method exhibit a complex structure with numerous pores and pits. The degree of surface complexity increases from the CORR_LOW (a) and LPBF_LOW (b) samples, through CORR_MEDIUM (c) and LPBF _MEDIUM (d), to the most complex surfaces for CORR_HIGH (e) and LPBF _HIGH (f).

Fig. 3 shows the percentage of NMPs for all tested samples depending on the lens magnification used. It should be noted that at higher lens magnifications, the number of NMPs decreases. NMPs are considered a good indicator of the ability of the measuring system used to correctly reflect the surface. At low magnifications (5×), the depth of field is significantly higher. The measurement algorithm has difficulty in precisely finding a single peak contrast height when multiple heights produce a similar focus signal. As a result, many pixels are dismissed as unmeasured because the focus signal is unclear and multimodal. At higher magnifications (20×, 50×), the DOF is significantly

narrower. This means that very clear, single-peak focus signals are obtained during the measurement process, resulting in a reduction in the number of NMPs. For the LPBF _HIGH sample, it was impossible to perform the measurement using a 50x lens due to the very small WD range of this lens. As expected, surfaces with higher complexity (CORR_HIGH, LPBF _HIGH) are more challenging to characterize accurately and therefore exhibit the highest number of NMPs. In contrast, smoother surfaces show a markedly lower proportion of NMPs, both for corroded samples and for those manufactured using the LPBF process.

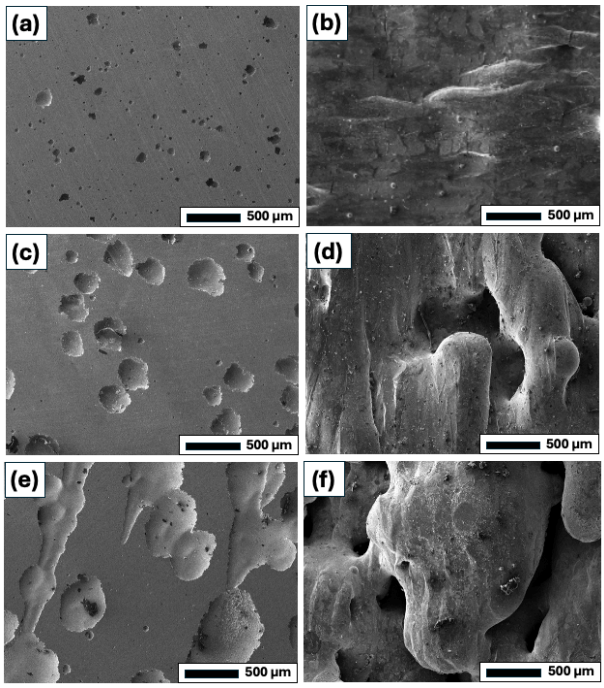

Figure 2. SEM images of the investigated surfaces – corroded samples (a, c, e) and LPBF samples (b, d, f) with low (a, b), medium (c, d) and high (e, f) porosity.

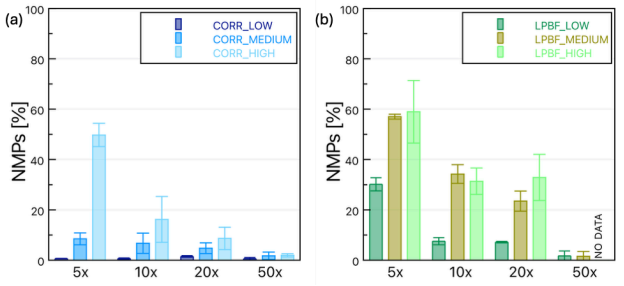

Figure 3. NMPs values for the corrosion-affected samples (a) and LPBF samples (b) for different objective lenses employed.

Fig. 4 and Fig. 5 show a summary of the basic roughness parameters - Sa and Sz, respectively. Tables (a) and (c) refer to samples subjected to corrosion degradation, while (b) and (d) refer to samples produced using the LPBF method. Tables (a) and (b) show the average value of the measurements performed, while (c) and (d) indicate the standard deviations obtained. It can be observed that as the magnification of the lens increases, the standard deviation values also increase, which is particularly evident for samples after corrosion degradation. This means that at high magnifications and the associated small imaging areas, the topographic data is very local and does not reflect the overall topography of the sample surfaces.

(a) Sa [µm]

MAGNIFICATION	CORR_LOW	CORR_MEDIUM	CORR_HIGH
5x	2,13	14,69	15,23
10x	1,81	11,92	29,72
20x	2,78	14,38	33,27
50x	0,98	14,92	18,40

(b) Sa [µm]

MAGNIFICATION	LPBF_LOW	LPBF_MEDIUM	LPBF_HIGH
5x	48,75	91,76	262,29
10x	33,54	69,85	198,81
20x	12,46	29,37	140,90
50x	6,63	24,27	NO DATA

(c) Sa deviation [µm]

MAGNIFICATION	CORR_LOW	CORR_MEDIUM	CORR_HIGH
5x	0,12	1,55	5,41
10x	0,34	7,79	5,42
20x	0,97	6,56	10,65
50x	1,25	12,65	12,52

(d) Sa deviation [µm]

MAGNIFICATION	LPBF_LOW	LPBF_MEDIUM	LPBF_HIGH
5x	4,43	7,87	56,33
10x	7,54	21,44	39,72
20x	7,60	15,33	58,43
50x	8,13	22,20	NO DATA

Figure 4. Average Sa parameter (a, b) and Sa standard deviations (c, d) heatmaps for the corrosion affected (a, c) and LPBF (b, d) samples.

(a) Sz [µm]

MAGNIFICATION	CORR_LOW	CORR_MEDIUM	CORR_HIGH
5x	100,20	131,56	144,33
10x	82,08	116,33	149,49
20x	88,25	105,76	132,85
50x	24,04	77,71	86,63

(b) Sz [µm]

MAGNIFICATION	LPBF_LOW	LPBF_MEDIUM	LPBF_HIGH
5x	560,08	781,69	1789,14
10x	264,56	489,49	1805,61
20x	105,00	313,61	1388,86
50x	43,69	53,05	NO DATA

(c) Sz deviation [µm]

MAGNIFICATION	CORR_LOW	CORR_MEDIUM	CORR_HIGH
5x	8,59	9,00	8,51
10x	5,36	9,77	18,68
20x	12,79	22,03	21,41
50x	8,45	47,12	52,71

(d) Sz deviation [µm]

MAGNIFICATION	LPBF_LOW	LPBF_MEDIUM	LPBF_HIGH
5x	23,21	46,98	235,95
10x	131,60	39,97	225,14
20x	47,08	100,00	210,60
50x	27,07	28,94	NO DATA

Figure 5. Average Sz parameter (a, b) and Sz standard deviations (c, d) heatmaps for the corrosion affected (a, c) and LPBF (b, d) samples.

When analyzing extensive surfaces, including those affected by degradation processes, it is important to quantitatively determine the ratio of pits to undamaged material. Standard height parameters such as Sa and Sz do not provide sufficient information about the distribution, quantity, and proportion of pits in the total topography under investigation. Fig. 6 shows a visual interpretation of the peak-hole analysis for a selected sample.

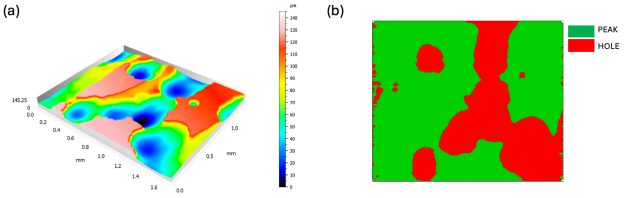

Figure 6. 3D surface topography visualisation for a CORR_HIGH sample with the 10x magnification objective (a) and peak-hole analysis for this surface (b).

A quantitative analysis of these observations is presented in Fig. 7 as a percentage indicator of the area of holes. Naturally, an increase in the percentage of holes was observed in samples from LOW to HIGH, both after the corrosion process and LPBF. For the 50x lens, the values obtained differ slightly from those for lenses with lower magnifications, and the standard deviations are large. These observations are consistent with the analysis of the height parameters Sa and Sz.

Considering the above observations, it is recommended to use lenses with magnifications of 10x and 20x for this type of measurement. They are the optimal choice in terms of the number of NMPs and the image size representing the topography under examination.

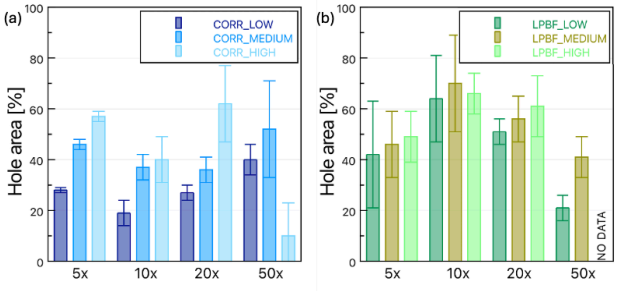

Figure 7. Hole area calculations for the corrosion-affected samples (a) and LPBF samples (b) for different objective lenses employed.

The parameters Vvc (core void volume) and Vvv (dale void volume) from ISO 25178 are particularly useful for surfaces with extensive pits, such as after pitting corrosion or LPBF printing, as they quantify the volume of voids rather than just height characteristics. Height parameters such as Sa or Sz ignore the number, size, and total capacity of the pits, for instance many small pits can result in a low Sa but a high Vvv. These parameters may indicate the functional properties of surfaces, such as their retention, liquid load-bearing capacity, and corrosion prediction. In the case of samples after corrosion degradation, lower Vvc and Vvv parameters were observed than for the samples produced using the LPBF method. It can be concluded that for samples subjected to corrosion processes, 10x and 20x lenses give comparable volume parameter values and similar standard deviation values. For LPBF samples, the use of a higher magnification lens gives slightly lower Vvv and Vvc parameter values. This may be a result of the smaller size of the observed area.

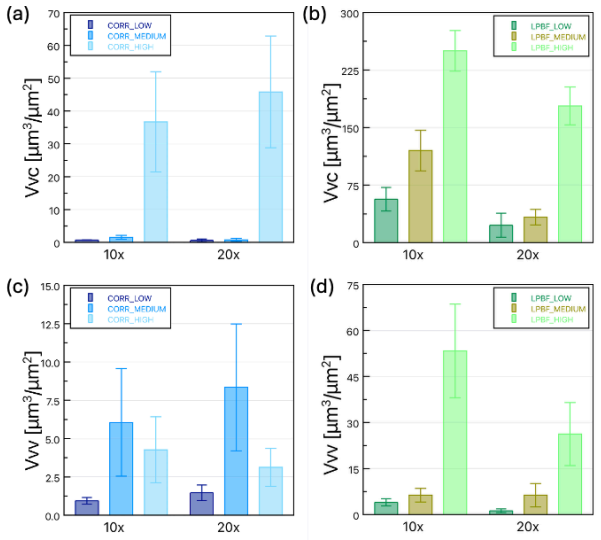

Figure 8. Vvc (a and b) and Vvv (c and d) values for the corrosion-affected samples (a and c) and LPBF samples (b and d) for two different objective lenses employed.

4. Conslusions

This paper presents a methodology for measuring and analyzing complex surfaces with a high degree of porosity, based on the example of surfaces after corrosion degradation processes and surfaces of samples produced using the LPBF method.

The influence of lens magnification in the FV method on the measurement results obtained was analyzed. At higher lens magnifications (20×, 50×), the number of non-measured points (NMPs) decreases significantly. This is due to a narrower depth of field (DOF), which provides clear, single-modal focus signals, eliminating the ambiguity that occurs at low magnifications (5×). More complex surfaces (CORR_HIGH, LPBF _HIGH) have the highest percentage of NMPs, indicating difficulties in accurately mapping highly developed topography. Smoother surfaces show a significantly lower proportion of NMPs for both corroded and LPBF -produced samples. The NMPs value is a reliable indicator of the measuring system's ability to accurately map surface topography. Minimizing NMPs by using the appropriate magnification is crucial for obtaining representative data on surfaces with complex pore and pit structures. Special attention should also be paid to the size of the imaged area. For high-magnification lenses, the size of the imaged area may be insufficient and may not represent the surface of the sample. Taking the above factors into account, magnifications of 10x and 20x are recommended for porous surfaces.

Selected height and volume parameters were analyzed. It was found that height parameters do not clearly reflect the degree of surface complexity, as they ignore the size, dimensions, and distribution of pores. Volume parameters such as Vvv and Vvc are more reliable indicators of surface quality. They can be supported by additional analyses, such as peak-hole surface analysis.

Acknowledgements

Financial support of these studies from Gdańsk University of Technology by the DEC-10/1/2025/IDUB/II.1b/Am grant under the Americium International Career Development - 'Excellence Initiative - Research University' program is gratefully acknowledged.

References

[1] Coelho L B, Kossman S, Mejias A, Noirfalise X, Montagne A, Van Gorp A, Poorteman M and Olivier M-G 2020 Mechanical and corrosion characterization of industrially treated 316L stainless steel surfaces *Surf. Coat. Technol.* **382** 125175

[2] Nugroho F A, Garhuom W, Andresen-Paulsen G and Ehlers S 2022 Numerical analysis of the correlation between the pitting severity and surface roughness of corroded specimens *Ships Offshore Struct.* **17** 2699–714

[3] Galati M, Minetola P and Rizza G 2019 Surface Roughness Characterisation and Analysis of the Electron Beam Melting (EBM) Process *Materials* **12** 2211

[4] Agrawal A K and Thoma D J 2022 High-throughput surface characterization to identify porosity defects in additively manufactured 316L stainless steel *Addit. Manuf. Lett.* **3** 100093

[5] Mirabal A, Loza-Hernandez I, Clark C, Hooks D E, McBride M and Stull J A 2023 Roughness measurements across topographically varied additively manufactured metal surfaces *Addit. Manuf.* **69** 103540

[6] Mendieta-Echevarría L, Sáenz-Nuño M A and Rubio E M 2025 Comparing the Effectiveness of R and S Roughness Parameters on Surfaces Lubricated with Standardized Nominal Particle Size Lubricants *Lubricants* **13** 148

[7] Anon ISO 25178-2: Geometrical Product Specifications (GPS) – Surface texture: Areal – Part 2: Terms, definitions and surface texture parameters.

[8] Walid A and Eifler M 2025 Common Practices and Methodologies in Scientific Functional Characterization of Surface Topography *Metrology* **5** 33

[9] Alar V, Razumić A, Runje B, Stojanović I, Kurtela M and Štrbac B 2025 Application of Areal Topography Parameters in Surface Characterization *Appl. Sci.* **15** 6573

[10] Tomkowski R, Xiaoyu Z, Leiro A and Archenti A 2022 Areal topography evaluation of a Ni-based alloy printed by electron beam melting (EBM) process European Society for Precision Engineering and Nanotechnology, Conference Proceedings: 22nd International Conference and Exhibition, EUSPEN 2022 (Geneva: euspen) pp 433–6

[11] Rojewski M 2026 Influence of digital optical microscope configuration and illumination conditions on the accuracy of surface roughness evaluation *Adv. Sci. Technol. Res. J.* **20** 406–22

[12] Mustafa A M, Muhamedsalih H, Tang D, Kumar P, Blunt L and Jiang J 2025 Investigation of focus variation microscopy immunity to vibrations *Precis. Eng.* **93** 87–98

[13] Rosentritt M, Schmutzler A, Hahnel S and Kurzendorfer-Brose L 2024 The Influence of CLSM Magnification on the Measured Roughness of Differently Prepared Dental Materials *Materials* **17** 5954